HTSC MICROBOLOMETER FOR PASSIVE MMW IMAGING APPLICATIONS

E. Zakar, D. Wikner, D. Potrepka, S. Tidrow, M. Dubey, K. Kirchner
Sensors and Electron Devices Directorate
U.S. Army Research Laboratory
Adelphi, MD 20783

ABSTRACT

High temperature superconductor (HTSC) microbolometers are highly sensitive thermal detectors that can be miniaturized for affordable passive millimeter-wave (MMW) imaging. When coupled to a micro-antenna and built into an imaging system, they are most promising for pilotage in fog, clouds, and smoke. A completely dry etch process is described for fabricating resistive-edge microbolometers based on $YBa_2Cu_3O_7$ (YBCO).

1. INTRODUCTION

Millimeter wave technology has unique qualities that make it ideal for "seeing through" poor visibility environments. Conditions that create poor visibility include low clouds, fog, smoke, dust, blowing sand, rain, and snow. Millimeter waves are naturally occurring forms of electromagnetic wave energy ranging from approximately 30 gigahertz (GHz) to 300 GHz, or 1 cm to 1 mm in wavelength. In comparison, light waves are found at roughly 500 to 1500 terahertz, or 600 to 200 nanometers in wavelength, in the electromagnetic spectrum. Because their wavelengths are large relative to the microstructure of most materials, millimeter waves tend to pass through most materials whereas light waves and infrared waves, which both have much smaller wavelengths, are not able to pass through many of these same materials. Just as regular cameras detect visible light energy and infrared cameras detect thermal energy in the infrared portion of the spectrum, millimeter wave cameras detect energy in the millimeter wave portion of the spectrum. Unlike regular cameras, however, passive millimeter wave rely on the energy being emitted from the objects in the scene (radiometric imaging) and require no external illumination, making the system entirely smaller.

The capability of MMW signals to penetrate obscurants has been well understood for a number of years, but implementing a real-time passive MMW imager in a cost effective system has been very challenging. Very creative solutions have been built by companies such as TRW, Trex Enterprises, Telaxis Communications, and Qinetiq (Moffa, 2000; Kolinko, 2005; Ewen, 2001; Anderton, 2006). Each of these systems has addressed the military user's desire to maximize the field of regard of the imager without adding excessively expensive or slow scanning mechanisms. This requires many thousands of detectors with corresponding RF MMIC circuits. These RF circuits usually include 40-60 dB of amplifier gain because the passive signal level is too low to measure directly with a standard MMW detector. The passive MMW signal power is on the order of 10 $pW/Hz^{1/2}$ and the required noise level of the detector is about 0.1 $pW/Hz^{1/2}$. This is well below the noise level of a standard detector. The result of all this is that the thousands of amplifiers in an imager end up dominating the cost of the entire system. Additionally, tightly packed arrays that use amplifiers need to be cooled to prevent overheating. These issues make it difficult to develop a passive MMW system that provides the Army user with cost-effective imaging capability.

One approach to this problem requires the development of more sensitive MMW detector devices. If a device or material structure can be found that enables one to detect passive MMW signals without RF amplification, the price of MMW imagers will drop dramatically, the weight and volume will decrease, and they will therefore become more useful for the military. Advancement in detector technology would also benefit the radar community by reducing the required transmitter power or by extending the dynamic range of the receiver. There are several approaches that can be used to improve detector sensitivity. Recent advances in room-temperature tunnel and Schottky diodes look very promising and may soon achieve a performance that enables them to image passive MMW signals (Lynch, 2006; Kazemi, 2005). For an even higher level of sensitivity, though, which is required for some applications, ARL is developing a liquid nitrogen cooled microbolometer detector. The high temperature superconductor YBCO experiences a very large change in resistance with a small change in temperature at the transition temperature between superconducting and non-superconducting (80-90 K). An airbridge bolometer structure can be built with YBCO that is coupled to a MMW antenna. Changes in the incoming MMW signal

Report Documentation Page

Form Approved
OMB No. 0704-0188

1. REPORT DATE	2. REPORT TYPE	3. DATES COVERED
01 NOV 2006	**N/A**	**-**

4. TITLE AND SUBTITLE	5a. CONTRACT NUMBER
HTSC Microbolometer For Passive Mmw Imaging Applications	5b. GRANT NUMBER
	5c. PROGRAM ELEMENT NUMBER
6. AUTHOR(S)	5d. PROJECT NUMBER
	5e. TASK NUMBER
	5f. WORK UNIT NUMBER
7. PERFORMING ORGANIZATION NAME(S) AND ADDRESS(ES) **Sensors and Electron Devices Directorate U.S. Army Research Laboratory Adelphi, MD 20783**	8. PERFORMING ORGANIZATION REPORT NUMBER
9. SPONSORING/MONITORING AGENCY NAME(S) AND ADDRESS(ES)	10. SPONSOR/MONITOR'S ACRONYM(S)
	11. SPONSOR/MONITOR'S REPORT NUMBER(S)

12. DISTRIBUTION/AVAILABILITY STATEMENT
Approved for public release, distribution unlimited

13. SUPPLEMENTARY NOTES
See also ADM002075., The original document contains color images.

14. ABSTRACT

15. SUBJECT TERMS

16. SECURITY CLASSIFICATION OF:			17. LIMITATION OF ABSTRACT	18. NUMBER OF PAGES	19a. NAME OF RESPONSIBLE PERSON
a. REPORT	b. ABSTRACT	c. THIS PAGE			
unclassified	**unclassified**	**unclassified**	**UU**	**6**	

Standard Form 298 (Rev. 8-98)
Prescribed by ANSI Std Z39-18

collected by the antenna heat up or cool down the bolometer and these small changes in temperature create measurable changes in the YBCO electrical resistance. Used in an array, this approach has the potential to produce very high quality MMW imaging without the use of RF amplifiers.

A MMW bolometer must be designed to minimize noise since the signal levels being measured are so small. One of the largest sources of noise in a bolometer is phonon noise created by thermal conduction. As RF energy makes the bolometer temperature different from its surroundings, thermal conduction increases causing phonon collisions in the structure that increase electrical noise. Phonon noise can be reduced by reducing the thermal conductivity between the bolometer and its surroundings. This is done by building the bolometer on an airbridge structure using materials that have a low thermal conductivity and by minimizing the dimensions of the airbridge legs. The baseline design for our YBCO bolometer is to build a small dimension airbridge with a length of 10 um and width of 3 um for just this reason.

The efficient capture of MMW energy in a bolometer requires that there be an antenna coupled to the bolometer. In a focal plane array system, the antenna dimensions are designed to be about equal to the diffraction limited beam spot in the image plane, as determined by the RF optics. The MMW energy collected by the antenna is then channeled to the bolometer, which has dimensions considerably smaller than a wavelength. The conduction of MMW energy through the bolometer material heats the bolometer, so efficient coupling of the antenna to the bolometer is required. Making a direct connection between the antenna and the bolometer can increase thermal conduction, so capacitive or inductive methods are used. A complete discussion of MMW bolometer design can be found in the reference (Nemarich, 2005).

Silicon micromachining is an important enabling technology of microsensors and devices for microsystems. It combines a variety of deposition, etching, and lithography processes that can make monolithic circuit integration affordable and miniaturized (Madou, 1997). These techniques can realize suspended transition edge bolometers by removing (releasing) the silicon substrate underneath the HTSC resistive area, thereby increasing the sensitivity, i.e. same as increasing the heating in the film by lowering the thermal conductance. At the same time the low thermal mass of the bolometers allow relatively fast (shorter than 0.5 ms) response times and enable video-frame-rate imaging. Several technical challenges must be overcome in order to fabricate HTSC microbolometers into efficient, low cost, and mobile platform systems:

- Growth of high quality, uniform 40nm thin film YBCO on silicon substrates
- Processing of the thin films without degrading the superconductor properties
- Etching methodology to create superconductor airbridges

2. RESULTS

2.1 Growth of YBCO on silicon

High quality growth of HTSC material on silicon is very difficult but we are collaborating with Neocera, Inc. that has pioneered Pulse Laser Deposition (PLD) techniques to grow thin films of YBCO on silicon substrates using epitaxial YSZ buffer layers. YBCO and silicon are chemically incompatible and require a lattice-matched buffer layer YSZ between the materials. The multilayer deposition sets stringent requirements for PLD but has some advantages: it works in high to low pressures, it gives good control of the stoichiometry of the deposited film, and allows easy and fast process handling. It is therefore an appropriate technique for in-situ preparation of heteroepitaxial multilayers. In spite of its advantages moderate surface quality of the as obtained thin films and small coverage area still remain the main obstacle of PLD to be used for device fabrication. The moderate surface quality has to do with outgrowths from known laser droplets (near spherical precipitates with diameter up to about 1um) that are slightly affected by the deposition parameters being an intrinsic characteristic of the PLD process (Boffa, 1995).

A multilayer PLD process was developed for growth of YBCO on silicon substrate. The deposition chamber was equipped with a multi-target holder for multilayer fabrication without breaking the vacuum (in-situ). Before deposition, silicon (100) oriented substrates with dimensions 10 mm×10 mm×0.5 mm were cleaned in acetone and ethanol with an ultrasonic cleaner. After the substrate was mounted on the heater using silver paste, the chamber was evacuated down to 1E(-8) Torr. The first layer YSZ was deposited by laser ablation using a 248 nm KrF excimer laser at a frequency of 5 Hz and beam fluence of 2.7 J/cm.^{2} The second layer YBCO was deposited using the same frequency but with a beam setting of 2.2 J/cm^2. When the final Au layer was deposited, the frequency was adjusted to 8 Hz and beam fluence to 3.1 J/cm.^{2} The Au layer was deposited in-situ to improve the electrical contact resistance and acts as a passivation layer during device fabrication and chemical processing. The PLD system was filled with oxygen to a pressure of approximately 200 mT during the YSZ and YBCO layer deposition cycles and evacuated during the Au cycle.

Material microanalysis and magnetic susceptibility measurements were performed on the PLD grown samples to determine the quality of the material. The chart in figure 1 shows the inductive response of the sample obtained in a magnetic susceptibility measurement. A thin film was placed in an oscillating magnetic field generated by a coil above the sample. A tiny sensing coil placed underneath the sample measured, for decreasing temperature, the decrease in the magnetic field there (due to increased shielding from the buildup of superconducting electron currents in the YBCO). As the YBCO cooled through the superconducting transition, this 'supercurrent' increased significantly and the magnetic field sensed by the pickup coil correspondingly dropped due to the decrease in strength of the YBCO's internal magnetic field. The field sensed then flattened out near a background value as temperature further decreased, indicating maximum supercurrent due to a strong transition of the YBCO film from a normal state to a superconducting state. The chart shows a sharp superconducting transition at 85-86 K, comparable to that for the best unpatterned YBCO films on YSZ/Si substrates (Mechin, 1997).

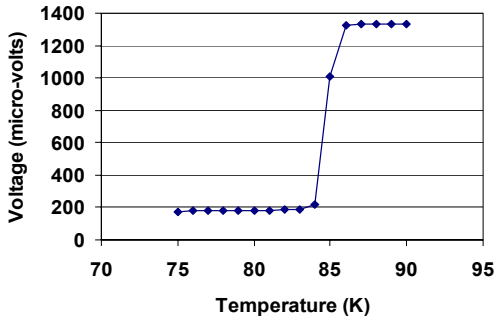

Fig. 1 Magnetic susceptibility measurement of PLD Au/YBCO/YSZ thin films on silicon.

X-ray diffraction (XRD) analysis was performed to determine the epitaxial quality of the grown YBCO material. Figure 2 shows a θ–2θ curve where the YBCO/YSZ thin films are well crystallized with single-crystalline-like structure and orientation. The YBCO thin film shows only (00*l*) peaks and no (*l*00) peaks are observed, suggesting that the YBCO thin film is uniformly *c*-axis oriented.

The surface topography of the deposited material shown in figure 3 was characterized by optical and scanning electron microscope (SEM). The optical surface scan reveals an average roughness height Ra=8 nm, a root mean square height Rq=11 nm, and average height plus the depth Rz=140 nm. Although the average roughness Ra=8 nm is relatively smooth compared to the YBCO film thickness (40 nm), the scale along the right hand side of figure 3 shows grains that protrude as high as Rz=140nm on the surface. A closer look over a surface area of approximately 60 x 80 um using the SEM reveals 0.5μm diameter outgrowths are distributed approximately every 2 μm^2 on the surface.

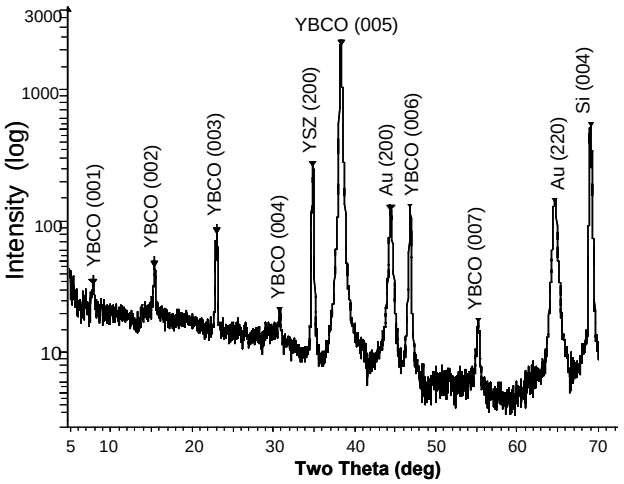

Fig. 2 XRD spectra of YBCO film on a YSZ buffered Si substrate. The (00*l*) peaks reveal the c-axis texture of the YBCO film and the (00*l*) oriented cubic structure of the YSZ layer.

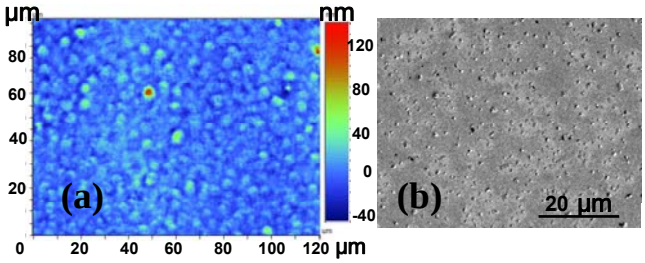

Fig. 3 Surface topography illustrated by (a) optical, and (b) scanning electron microscope.

2.2 Processing and fabrication

An etching process for creating a superconductor airbridge thermally isolated from the silicon substrate has been demonstrated using a combination of ion beam etching (IBE) and reactive ion etching (RIE) as illustrated in figure 4. We designed a set of material processing and fabrication procedures using completely dry chemical etching that preserved the HTSC properties. This is an improvement over conventional selective wet chemical etching techniques that are both harsh on the YBCO and require additional complex alignment steps to the substrate material (Rice, 1998) leading to very poor device yields. Conventional wet etch technology alters the HTSC properties, and typical reactive dry etching of YBCO is very complex due to

itsstrong chemical bonds and very low vapor pressure of the etched species that causes redeposition. Improvements in equipment and advancements in thin film patterning processes have been designed to pattern small dimension airbridges with a length of 10 um and width of 3 um following these basic steps:

- Au(100nm)/YBCO(40nm)/YSZ(150nm) fig. 4a.
- Photolithography mask pattern - bridge structure.
- Ion beam etching down to silicon fig. 4b.
- Photolithography mask pattern - silicon trench.
- Isotropic etching of the silicon - airbridge fig. 4c.
- Ion beam etching of Au passivation fig. 4d.

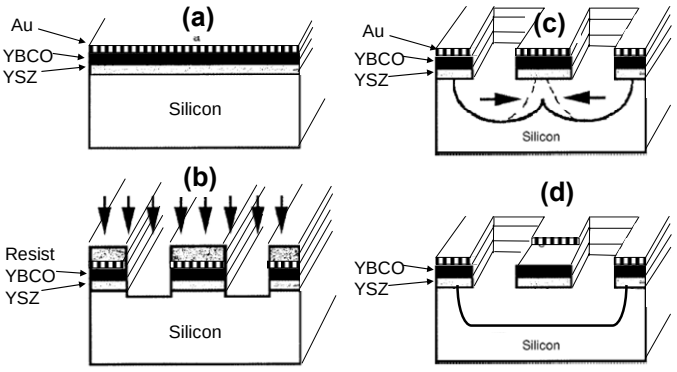

Fig. 4 A drawing of the basic steps depicting the fabrication of a microbolometer structure.

The YBCO thin film material in figure 4a is under mechanical stress and must be less than 50 nm thick to avoid cracking (Fenner, 1991). IBE was chosen for patterning of the film over conventional RIE and wet etching because it has an overwhelming advantage of etching very straight lateral features. A benefit of Au on top the YBCO is that it acts as a passivation layer and prevents the alteration of the HTSC properties during photolithography processing and chemical etching (Khrebtov, 2004). An Au layer over the entire YBCO layer can reduce the electrical noise level during device testing. McDonald, et al. (McDonald, 1999) found YBCO thermometers for a microbolometer device were electrically sensitive to their passivation layer which raised the noise in the films by about a factor of 100. The alternative was to first cap the YBCO with Au for passivation followed by adding an insulator for electrical isolation.

2.3 Etching

The etching rates for Argon IBE at 500v, 20 deg incidence angle, and 1mA/cm for the materials Au, YBCO, YSZ, and Si are summarized in Table 1.

Table 1 Ion beam etch rates of the different material layers in the HTSC stack.

Material	Thickness (μm)	Etch Time (min)	Etch Rate (μm/min)
Au	0.10	1.0	0.1
YBCO	0.04	2.0	0.02
YSZ	0.15	8.8	0.017
Si	0.25	3.5	0.07

Challenges during ion beam etching were**:** (a) irregular shaped bridge dimensions due to lateral erosion of the photoresist mask, (b) build-up of material on the etched pattern side walls (redeposition) that can cause electrical shorts between the layers, and (c) overetching or "trenching" below the baseline of the substrate surface. Etching directly into the material produced trenching in the silicon substrate due to the increased collision activity at the intersection of the mask sidewall and base of the material. To avoid trenching we did not etch directly into the material, but at an incidence angle beyond 5 degrees. The bridge design width of 3 um was achieved during the patterning in figure 4b, but surface irregularities similar in size and location to the outgrowths from the original grown surface transferred down to the silicon surface level (figure 5a). The density of protrusions acted as a screen and prevented the patterning of the silicon trench by RIE using SF_6 plasma. In order for the SF_6 plasma to penetrate through to the silicon as shown in figure 4c required the elimination of the surface protrusions. We overcame the obstacle by overetching until the silicon surface became smooth and free from protrusions. The drawback was that redeposition occured on the etched sidewall features and the photoresist mask became very difficult to remove**.** Figure 5b shows a patterned feature with the scaly looking photoresist still intact. The photoresist was eventually removed by dry oxygen plasma at twice the normal power and etching time used for standard exposed resist. No harm was done to the surface of the YBCO because of the Au passivation layer.

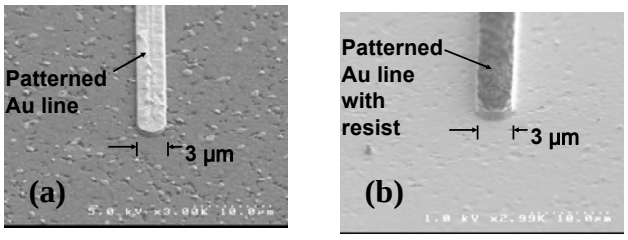

Fig. 5 SEM image of (a) rough silicon surface after IBE, and (b) smooth silicon surface after the over etching. In fig. 5b the photoresist mask on top of the patterned 3 um-wide line feature has not yet been removed to illustrate the tough and scaly surface features.

An airbridge was demonstrated by isotropically etching a silicon trench underneath the previously patterned line structure as shown in figure 6. The length of the bridge was determined by a mask pattern spacing of 10 um. Undercutting is an integral part of the isotropic etching mechanism that allowed both etching and removal of the silicon material underneath the HTSC line structure, a process most often called a 'release'. In isotropic etching, the amount of material removal is uniform in all directions. Although the photoresist mask pattern spacing theoretically determines the bridge length, the nature of isotropic etching causes the actual HTSC line to be longer. In figure 6 the etched depth is 5 um and the undercutting is nearly 4 um on both sides of the bridge, making the total length of the bridge 19 um after the resist is eventually removed. The silicon etch rate by RIE in SF_6 was 0.5 um/min when the mask window was 10 um wide. The amount of silicon etched was complex and depended on the amount of silicon area exposed by the mask dimensions and etch chemistry recipe.

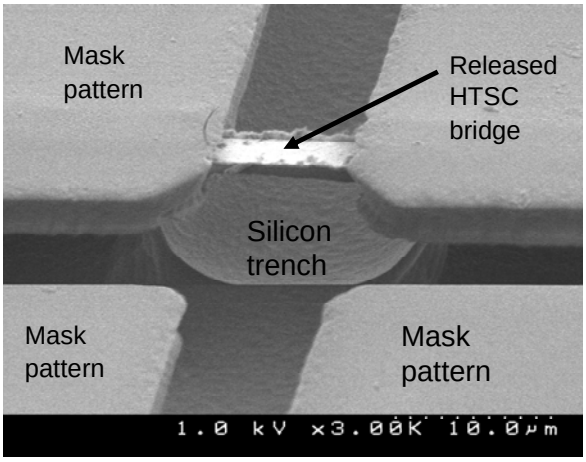

Fig. 6 HTSC airbridge structure over the isotropically etched silicon substrate.

The final process step illustrated in figure 5d required the removal of the Au passivation layer by IBE to expose the active YBCO resistor design dimension, which was accomplished with the same mask pattern. The Au was completely removed in approximately 1.5 minutes. The etching was partitioned into several sequences and inspection conducted in between to prevent over etching into the YBCO layer. Material redeposition is still evident along the edges of the bridge after the Au removal but can be prevented by taking additional preventative measures during the first patterning process step.

CONCLUSIONS

We successfully demonstrated the release of a HTSC bridge and showed the resilience of this structure to a highly energetic IBE process. A completely dry etching process was developed that can be used to fabricate miniaturized HTSC bridges several microns in dimension. A refinement in the etching process will lead to better control and possible elimination of the redeposition material along the length of the bridge. The etch depth and lateral dimension of the bridge can be further controlled by timing the etching period, and by adjusting the mask pattern spacing. The surface of the etched silicon trench is very smooth using RIE with SF_6 plasma. The fabrication progress reported here makes closer the realization of a high fidelity detector for millimeter-wave imaging. The successful development of this type of detector will lead to cost-effective detector arrays and imagers for advanced "see-through" technology.

AKNOWLEDGEMENTS

The authors gratefully acknowledge Richard Piekarz and Derwin Washington for developing a reliable lithography process, John Conrad for ion beam etching, Michael Derenge for knowledge and discussions on use of 3-D optical metrology techniques, and Jeff Pulskamp for the CAD layout and mask design verification at the ARL.

REFERENCES

Anderto R. N., May 2006: Security scanning at 94GHz, Proceedings of the SPIE, Vol. 6211.

Boffa, V. 1995: High-quality surface YBCO thin films prepared by off-axis pulsed laser deposition technique, Physica C 241, pp. 30-36.

Ewen, D., August 2001: Flight test of a MMW imaging radarometer , Proc. of the SPIE, 4373, pp. 24-34.

Fenner, D.B., March 1991: High critical currents in Y-BA-CU-O films on silicon using YSZ buffer layers, IEEE Transactions on Magnetics, 27 (2): 958-965 part 2.

Kazemi H., May 2005: First MMW characterization of ErAs/InAlGaAs/InP semimetal-semiconductor-Schottky diode (S^3) detectors for passive millimeter-wave and infrared imaging, Proceedings of the SPIE, Vol. 5789.

Khrebtov I. A. and Tkachenko A. D., March 2004: High-temperature superconducting bolometers based on silicon-membrane technology, J. Opt. Technol. 71 (3), pp. 143-152.

Kolinko V. G., May 2005: A passive millimeter-wave imaging system for concealed weapons and explosives detection, Proceedings of the SPIE, Vol. 5781, pp. 85-92.

Lynch, J. 2006: Unamplified direct detection sensor for passive millimeter wave imaging, Proceedings of the SPIE, Vol. 6211, May.

Madou, M.,1997: The Fundamentals of Microfabrication, CRC Press, New York.

McDonald D.G., et al., 1999: Passivation, transition width, and noise for YBCO bolometers on silicon, IEEE TRANSACTIONS ON APPLIED SUPERCONDUCTIVITY 9 (2): 4471-4474, Part 3.

Mechin, L., May 15 1997: Suspended epitaxial YBaCuO microbolometers fabricated by silicon micromachining: Modelingand measurements, Journal of Applied Physics, 81 (10), 7039-7047.

Moffa P., 2000: Passive millimeter-wave camera flight tests, Proceedings of the SPIE, Vol. 4032, July, pp 14-21.

Nemarich J., March 2005: Microbolometer Detectors for Passive Millimeter-Wave Imaging, Army Research Laboratory Technical Report, ARL-TR-3460.

Rice J.P., 1998: High-Tc superconducting antenna-coupled microbolometer on silion, SPIE, 2159, pp. 98-108.